

Properties of Nanotitanium for Potential Medical Applications

Halina Garbacz,* Krzysztof Jan Kurzydowski

Summary: Two titanium-Grade2 (a coarse-grained in the received state and nanostructured after hydrostatic extrusion) were examined wear and corrosion tests. Passive oxide layers formed on the surface of both materials had a thickness of about 6 nm and the same chemical composition. The corrosion resistances measured in a 0.9% NaCl solution were comparable. The friction tests show that nano-grained Ti is suitable for use in the tribological pair with UHMWPE.

Keywords: implants; nanotechnology; structure-property relations

Introduction

Titanium exhibits excellent physical and chemical properties. It has a good biocompatibility and biointegration with the human body. When it is in the coarse-grained form, its yield point is however too low to be used for implants. The TA6V alloy, which is widely used in medical applications, is two times as strong as pure titanium, but the vanadium and aluminium atoms present in this alloy reduce its biocompatibility. The aim of the present work was to examine the properties of nano-grained titanium obtained by hydrostatic extrusion (HE), whose strength is higher than that of the conventional TA6V alloy thanks to the greater number of grain boundaries. HE belongs to the methods of severe plastic deformation (SPD) and yields homogeneous, fully dense bulk nano-metals such as aluminium alloys, nickel and titanium.^[1–6]

Bearing in mind possible future applications of nano-titanium, it is important to examine its utility properties. This study presents the results of examination of the wear resistance and corrosion resistance of nano-titanium (Ti-Grade 2), produced by hydrostatic extrusion.

Experimental Part

The material examined in the study was Ti-Grade2 (grain size $\sim 21 \mu\text{m}$), subjected to multistage HE at room temperature. The samples had the form of rods. The details of the HE process were reported earlier.^[4] It has been found that the HE process results in a substantial refinement of the titanium microstructure. After HE, the titanium rods had an average grain size of about 90 nm (Figure 1). The refinement of the microstructure was accompanied by an improvement of the mechanical properties of titanium, such as microhardness and tensile strength, with the good plasticity of the initial material being preserved. The tensile strength of the nanotitanium was 1100 MPa, the microhardness - 273HV0.2, and the elongation - about 10%.

The surface microstructure and certain selected properties of untreated titanium and HE-treated titanium were examined using various analytical techniques. The Ti samples were examined by Auger Electron Spectroscopy (AES) to determine the composition and estimate the thickness of the passive surface film. The elements present in the oxide layer and its chemical composition were determined using a Microlab 350 (Thermo VG Scientific) analytical instrument. An Ar^+ ion gun was used to measure the composition profiles of the film. Discontinuous sputtering (time steps of 6 s)

Warsaw University of Technology, Faculty of Materials Science&Engineering, 02-507 Warsaw, Woloska 141, Poland
E-mail: haga@inmat.pw.edu.pl

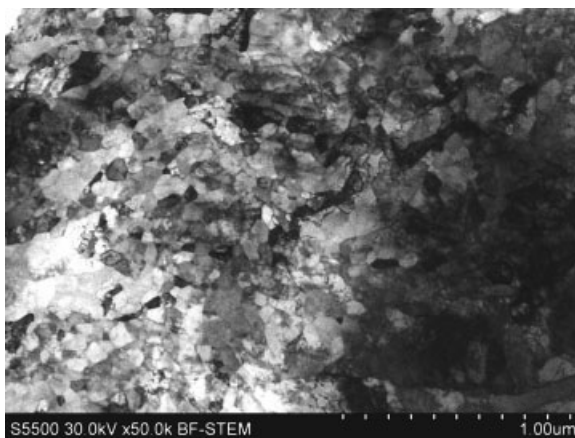


Figure 1.

Microstructure of Ti-Grade2 after hydrostatic extrusion (SEM/STEM Hitachi S 5500).

was used to remove gradually the oxide film. The sputtering parameters were: (a) ion energy 3 keV, (b) beam current 1 μA , and (c) the crater size 2×2 mm. After each sputtering period, the Auger spectra were recorded at $E_p = 10$ keV. An Advantage-based data system software was used for data acquisition and processing.

The tribological tests were performed using a T-11 rotating pin-on-disc tribometer with a fixed pin. The pin wear volumes were calculated according to the ASTM pin-on-disc test method G-99.^[7] The cylindrical pins (3.0 mm in diameter) were made of titanium in the initial state and of nano-titanium processed by HE. The friction tests were performed against an ultra-high molecular weight polyethylene (UHMWPE) disc in ambient air. The sliding speed was about 0.15 ms^{-1} . The normal loads were varied from 2 and 15 N, so as to establish two fixed values of the mean pressure at the interface: 0.75 and 2.0 MPa. In each test, the sliding distance was 540 m. The tests were carried out in a normal saline solution (0.9% NaCl). During the test, the changes of the friction coefficient were measured. The total linear wear rate, including both the decrease of the pin height and the depth of the wear track on the disc, was estimated during the test using a capacitive displacement sensor. The wear rates were also

calculated from the weight loss Δm of the titanium pins.

Corrosion tests were carried out in a 0.9% NaCl solution for 20 h. Changes in the character of the corroded layer were analyzed by the impedance spectroscopy method. The impedance tests were conducted using an Autolab PGSTAT100 computerized system (voltage signal amplitude - 20 mV, frequency - 1 MHz – 0.001 Hz, the reference electrode - a saturated calomel electrode (SCE)). The potentiodynamic tests were conducted by polarizing the samples at a potential variation rate of 0.2 mV/s.

Results

SPD processes applied to metals and alloys transform their structure into a nanostructure, thereby improving significantly their mechanical properties. The tensile strength of nano-titanium obtained by the HE method is comparable with that of the TA6V alloy. There are no however reports in the literature describing the effect of the SPD processes on the microstructure and the phase composition of the layers present on the surface of the nano-materials, whereas the presence of oxide layers affects many properties of the material, such as the wear and corrosion resistance, properties

essential from the point of view of bio-medical applications.

The passive surface films formed on the Ti samples were examined by Auger Electron Spectroscopy (AES). By way of example, Figure 2 shows the spectra obtained for a Ti sample before (a) and after HE (b). We can see that the O (KLL) peak disappears in the course of sputtering, which is in agreement with the analytical results obtained at various depths of the sample: from within the passive film to,

eventually, within the substrate. After sputtering, in the region of the oxide film far away from the substrate, the spectra revealed the presence of metallic Ti (LMM).

Three distinct domains can be distinguished within the profile obtained for Ti (Figure 3): I – a contaminated oxide film (zone which is enriched with carbon), II – an anodic oxide film containing Ti^{ox} , and III – the substrate containing Ti^{m} . A careful inspection of the composition profiles reveals that the oxide films are very thin.

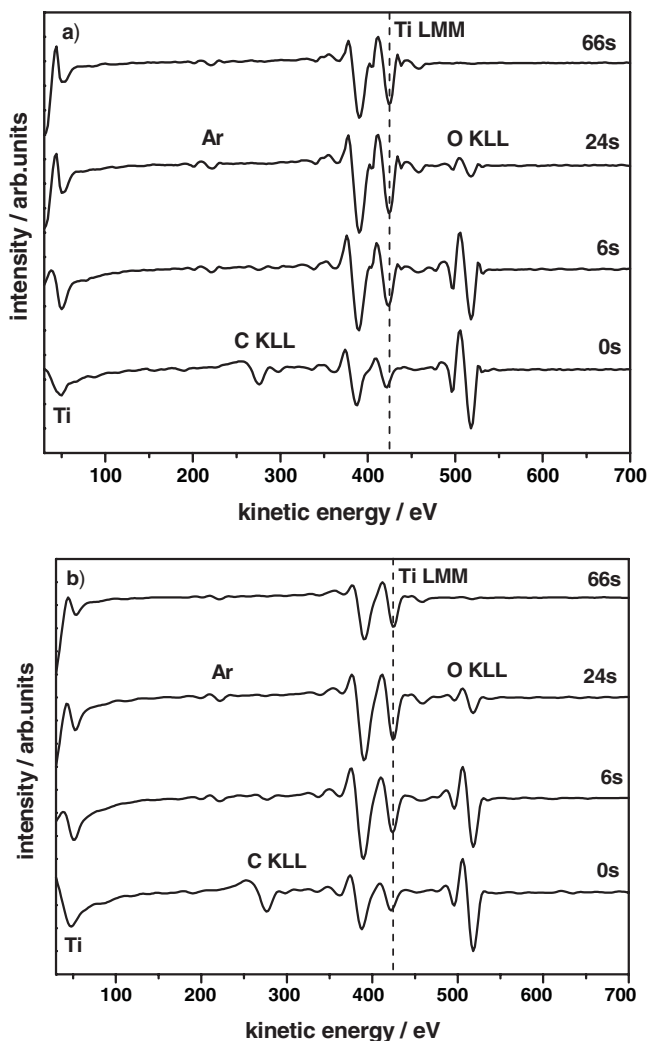


Figure 2.

Differential ($\text{dN(E)}/\text{dE}$) Auger spectra obtained for Ti samples (a) in the initial state, (b) after HE, measured at various depths of the thin passive film (from the oxidized state to the metallic substrate) during the sputtering.

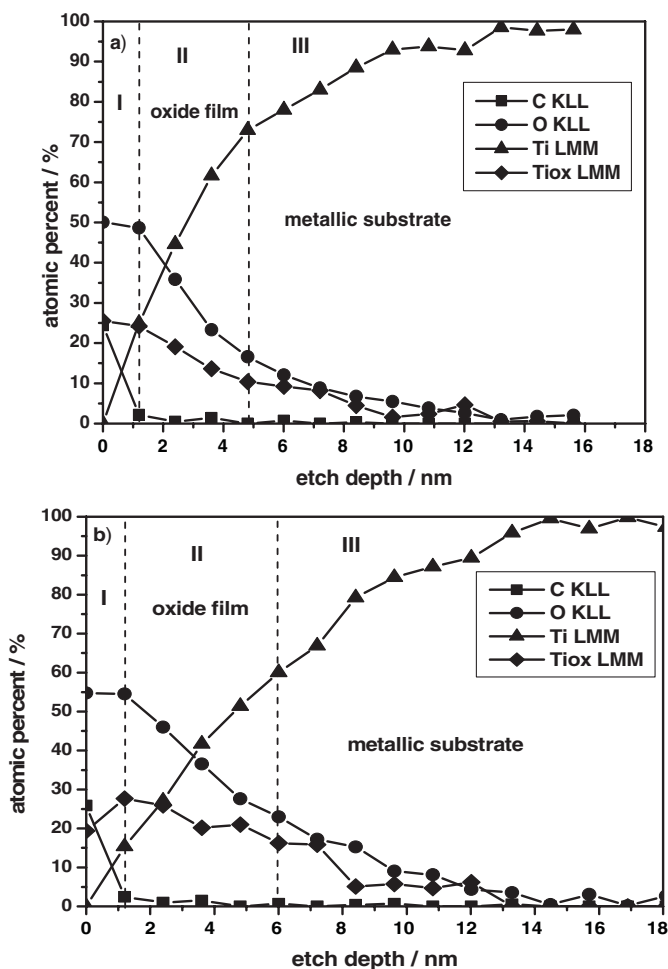


Figure 3.

Chemical composition profile of an air-formed oxide film on Ti samples (a) in the initial state, (b) after HE showing the three regions: I – contamination oxide film, II – oxide film, III – metallic substrate (Ti). Atomic percent values were calculated from the integral spectra.

The Ti^{ox} and O signals are only stable at the beginning of the profiles. The ratio of Ti^{ox} (LMM) to O (KLL) measured within the oxide film (region II), undergoes changes during the sputtering. These results show that, in both materials, the sputtering (t_{sputt}) time necessary to remove the oxide film are very similar (24 s – initial state, 30 s – HE). The t_{sputt} (etch depth) estimated from the composition profiles corresponds to ~66% of the maximum value of the O (KLL) signal. Hence, we can see that the thicknesses of the two films are almost the same

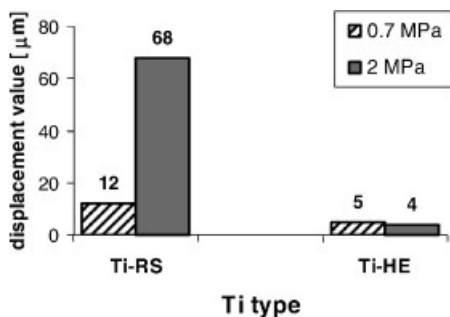
(5 nm on Ti in the initial state and 6 nm on HE-treated Ti).

This study also presents the investigation results of the wear resistance and corrosion resistance of Ti-Grade 2 nanotitanium obtained by hydrostatic extrusion. No measurable weight loss of the titanium pins was observed during the wear tests against UHMWPE (Table 1). The displacement values, which are the total of the UHMWPE disc wear, and the plastic deformation of titanium pins, were on a low level (Figure 4). The differences in the displace-

Table 1.

Results of tribological tests obtained during dry sliding against UHMWPE disc, $p = 2$ MPa (Δl -differences in displacement values, Δm -weight loss, μ - friction coefficient, Ti-RS- titanium in as received state, Ti-HE- titanium after HE).

Counter specimen material	Δl		Δm		μ	
	[μm]		[mg]		[-]	
	Ti-RS	Ti-HE	Ti-RS	Ti-HE	Ti-RS	Ti-HE
UHMWPE	68	4	0	0	0.07	0.09

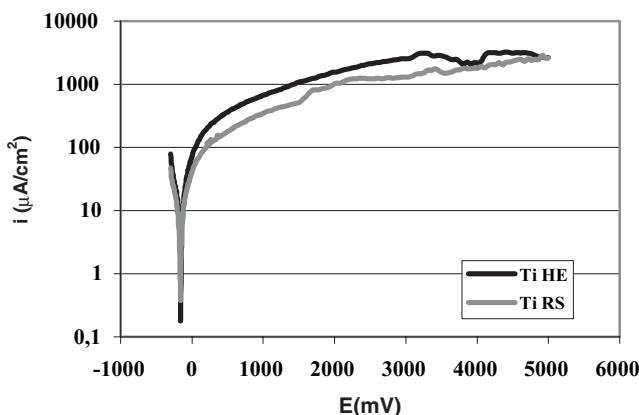
**Figure 4.**

Comparison of the displacement values obtained during tests with the counterspecimen made of UHMWPE and with mean pressure 0.7 and 2 MPa.

ment values show how favorably the HE process affects titanium properties. This indicates that, nano-grained Ti can be used in the tribological pair of an implant into the human body.

The corrosion resistance values of the processed titanium were measured after about 20 hours of exposure in a 0.9% NaCl solution. The corrosion potential values were calculated from the anodic polarization curves (Figure 5). Titanium samples, both in the initial state and that after extrusion, showed a comparable corrosion resistance. None of them underwent pitting corrosion, but only uniform corrosion occurred. This observation was confirmed by examination of the surfaces of the samples in an optical microscope. The values of the corrosion potentials and corrosion current densities obtained for the samples before and after extrusion were found to be comparable.

The results obtained for HE-treated samples indicate that the surface of the passive layer formed on the deformed metal is more developed compared to that of the sample in the initial state.^[8] It should be noted that all the samples intended for

**Figure 5.**

Anodic polarization curves obtained for Ti prior and after HE in 0.9% NaCl; i - current density, E - potential.

the corrosion tests were subjected to the same preparatory procedure. Hence, the higher surface development may be attributed to nanocrystalline structure of this material, i.e. to the greater number of grain boundaries and their influence on the diffusion processes that take place during the formation of the passive film.

Conclusion

The thickness of the passive oxide film formed on the titanium surface appears to be independent of the grain size of the titanium substrate: both on the surface of the nano-Ti samples and of the untreated -Ti samples, the oxide layers are about 6 nm thick and have the same chemical composition.

Nano-Ti shows good corrosion resistance in 0.9% NaCl solution and shows no tendency to pitting corrosion.

The results of friction tests performed with an UHWMPE counter-specimen indicate that the HE process has a favorable effect on titanium properties. This tribolo-

gical pair can be recommended for use in implants into the human body in medical applications.

Acknowledgements: The work was supported by the Polish State Committee of Scientific Research (Project No T08A 019 29). The authors wish to express their thanks to Dr. M. Grądzka-Dahlke and Dr. M. Pisarek for their valuable assistance in the measurements of the wear resistance and in identification of the components of the oxide films.

- [1] R. Z. Valiev, R. K. Islamgaliev, I. V. Alexandrov, *Progress in Mat. Sci.* **2000**, 45, 103.
- [2] V. M. Segal, *Mat. Sci. Eng.* **1995**, A 197, 157.
- [3] M. Richert, Q. Liu, N. Hansen, *Mat. Sci. Eng.* **1999**, A 260, 275.
- [4] H. Garbacz, M. Lewandowska, W. Pachla, K. J. Kurzydłowski, *Journal of Microscopy* **2006**, 223, 272.
- [5] M. Lewandowska, H. Garbacz, W. Pachla, A. Mazur, K. J. Kurzydłowski, *Sol. St. Phen.* **2005**, 101, 65.
- [6] K. J. Kurzydłowski, *Mat. Sci. Forum* **2006**, 503–504, 341.
- [7] Standard Test Method G-99-95a. “ASTM Annual Book of Standards”, Vol. 03.02, American Society for Testing and Materials, West Conshohocken, PA **1999**, pp. 401–405.
- [8] H. Garbacz, M. Pisarek, K. J. Kurzydłowski, *Biomolecular Engineering* in press.